https://doi.org/10.20965/jrm.1996.p0252

Paper:

Servo System Design Considering Low-Stiffness of Robot

Akira Shimada

Seiko Seiki Co., Ltd.
4-3-1 Yashiki, Narashino, Chiba, 275 Japan

[Received January 8, 1996; accepted January 22, 1996]

This paper describes the practical design method of an advanced servo system for industrial robot manipulators, *where it includes a disturbance and velocity observer.* It is first assumed that the feature on frequency response of the robot is approximated to the feature of two-mass mechanism. Actually this is confirmed by some experiments. On the other hand, it is insisted that the actual servo system should be simple for industrial use. The observer is designed for the load which has the feature of single moment of inertia. Based on the assumption that there is a difference between these features, it is introduced that the servo system can be effectively used if only the qualified gains are selected considering low-stiffness. The special relation between the frequency *analysis and the pole allocations are then shown, and* Finally the experimental results are introduced.

Keywords: Observer, Disturbance, Velocity, Robot, Servo, Low-stiffness

1. Introduction

Robots for industrial use are used in a wide range of application in the industrial field. Some of them are required to have a long stroke or a payload. For instance, there is a handling robot which moves around in the semiconductor plant as installed on an automatic guided vehicle. However, the composition of such mechanisms tends to be low in stiffness and deterioration in kinetic performance is liable to occur. The fluctuation in inertia and friction interfere with the determination of a highly accurate position. In actuality, when the frequency characteristics of the robots for industrial use with a low stiffness are measured, it is quite often that they exhibit characteristics close to the two-mass mechanism. In this report, a method will be proposed to improve the characteristics of motion of such robots for industrial use. The people concerned, including the author, have hitherto made a proposal on the least dimension observer to estimate disturbance and kinetic velocity, assuming the object of control as the single inertial load.[1,2] The subject observer is identical with the disturbance observer[3] popularly known in principle, but it differs from the latter in that it estimates the kinetic velocity simultaneously for use in controlling. Thus, it is called the disturbance-velocity estimated type servo system and is set apart from the rest. Consequently, a proposal will be made for a guideline in design of low-stiffness loads of the above-mentioned servo system as follows.[4]

1) The transfer function on the primary side of the two-mass mechanism has poles with resonance characteristics and a zeros with anti-resonance characteristics. When an attempt is made to feed back the estimated disturbance data and control the resonance poles and the zeros completely, the resonance characteristics on the secondary side will be conspicuous.[5] It will be indicated that this phenomenon occurs in case of the subject observer and the cause and the method of dealing with the situation will be observed. As the next step, the selection of nominal inertia data used in the design of the control system will be examined, and it will also be shown that the compensator on the external side of the observer likewise requires an observation pertaining to resonance characteristics. In conclusion, qualified gains of both the observer and the compensator can be obtained.

2) Friction is regarded as an unknown constant disturbance. As a result, the control system is required to be of more than one type based on the internal model principle. The disturbance-velocity estimated type servo system already includes a compensator for stabilization of one type.

3) Improvement in traceability is made to come under the feed-forward item of acceleration.

4) Finally, experimental results based on analytical results will be introduced. In the course of experiments, the acceleration at the tip of the robot and the position deviation of the motor shaft will be evaluated. This is due to the fact that the former is translated as the acceleration on the secondary side of the two-mass mechanism and the latter, as being equivalent to the position deviation on the primary side.

2. Models of Control Objects

In the following will be discussed the case of a specific

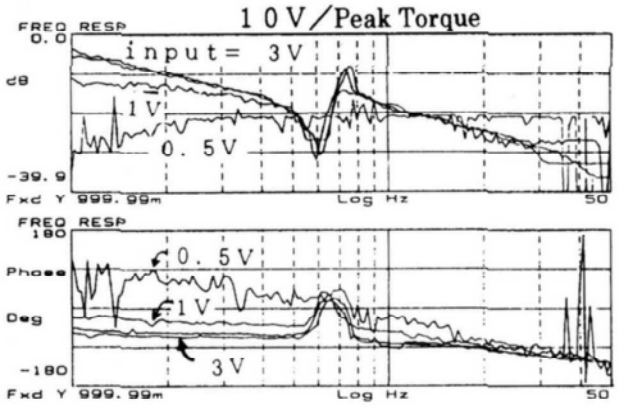

Fig. 1. Bode diagram for some torque inputs.

drive shaft of robot manipulation similar to a load model of the two-mass mechanism. However, there is a non-linear friction on each shaft and there appear different frequency characteristics as the torque input amplitude changes. The inputs shown in **Fig.1** are torque commanded, while the outputs show motor velocities. The motor drive circuit consists of the electric control systems with a response frequency of 2kHz to generate a drive torque in proportion to the torque command. Low gain characteristics are shown in the entire bands in Fig.1 against the inputs of small amplitudes and the points of resonance are not clear. As the input amplitude grows larger, both anti-resonance characteristics and resonance characteristics become conspicuous. The phase reaches close to −90°, and typical characteristics unique to the two-mass mechanism appear. In addition, the inertia on the secondary side of the two-mass mechanism fluctuates in accordance with the posture of the robot and the object it holds. Frequency characteristics also change. **Figure 2** presents examples of actual measurement. The transfer function models of the two-mass mechanism are shown in Eqs.(1) through (4) and a block diagram is as shown in **Fig.3**. Wherein, max inertial sum = J_{max} (· = $J_1 + J_{2max}$), resonance frequency = ω_1 Anti-resonance frequency = ω_2, attenuation coefficient = ξ_1, ξ_2, inertia on primary side = J_1 inertia on secondary side = J_2, elasticity = k, Viscosity = d, non-linear friction and gravity are regarded as unknown disturbances and expressed as T_{d1} and T_{d2}, respectively. Corresponding numerical values have been entered to obtain **Table 1**.

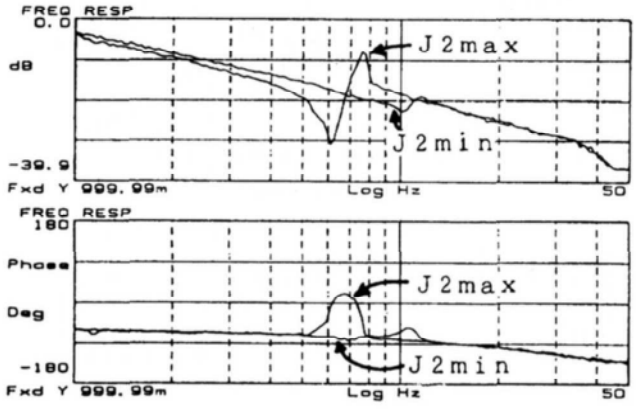

Fig. 2. Bode diagram example for change of pose.

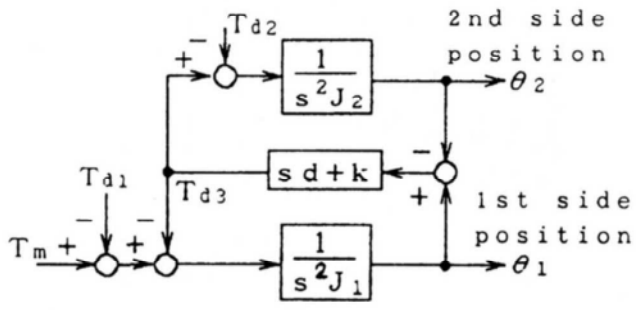

Fig. 3. Model of 2-mass system.

$$\frac{\theta_1(S)}{T_m(s)} = \frac{1}{s^2(J_1+J_2)} \frac{s^2J_2 + sd + k}{s^2J_1J_2/(J_1+J_2) + sd + k} \quad \cdots\cdots (1)$$

$$\frac{\theta_2(S)}{T_m(s)} = \frac{1}{s^2(J_1+J_2)} \frac{sd + k}{s^2J_1J_2/(J_1+J_2) + sd + k} \quad \cdots\cdots (2)$$

From the Eq.(1), the following equations can be obtained:

$$\text{Resonance } \omega_1 = \sqrt{\frac{k}{J_1J_2/(J_1+J_2)}} \quad \cdots (3)$$

$$\text{Anti-resonance frequency } \omega_2 = \sqrt{\frac{k}{J_2}} \quad \cdots (4)$$

3. Disturbance/velocity Observer

The procedures for designing the disturbance/velocity observer are as follows.[1)]

The object of control at the time of designing is expressed as follows.

$$T_m = J_0\ddot{\theta}_1 + T_d \quad \cdots\cdots (5)$$

Where, nominal inertia: J_1, Position: θ_1, drive torque: T_m, disturbance torque: T_d, on the assumption that $dT_d/d\,t = 0$, the situational Eqs.(6) and (7) are obtained.

$$\begin{bmatrix}\dot{\theta}_1\\ \ddot{\theta}_1\\ T_d\end{bmatrix} = \begin{bmatrix}0 & 1 & 0\\ 0 & 0 & -1/J\\ 0 & 0 & 0\end{bmatrix}\begin{bmatrix}\theta_1\\ \dot{\theta}_1\\ T_d\end{bmatrix} + \begin{bmatrix}0\\ 1/j\\ 0\end{bmatrix}T_m \quad \cdots\cdots (6)$$

$$\theta_1 = [1\ 0\ 0]\ [\theta_1\ \dot{\theta}_1\ T_d]^T \quad \cdots\cdots (7)$$

Because it is an observable measurement, the gopinath

Table 1. Fluctuation range example of parameters.

Item	Range of fluctuation
Total mass $J=J_1+J_2$	1.38-1.64×10^{-4} kgm²
1st mass J_1	1.25×10^{-4} kgm²
2nd mass J_2	0.15-0.39×10^{-4} kgm²
Inertia ratio α	0.12-0.31
Stifness k	0.059 1 Nm/rad
Damping d	1.244×10^{-4} Nms/rad
Resonance freq. ω_1	7.1-$10.6\times2\pi$ rad/s
Anti-resonance freq. ω_2	6.2-$10.0\times2\pi$ rad/s
Resonance ratio β	0.87-0.94
Coulomb friction f	0.023 1 Nm

type minimal order state observer Eqs.(8) and (9) are obtained. [1)]

$$\begin{bmatrix} \dot{z}_1 \\ \dot{z}_2 \end{bmatrix} = \begin{bmatrix} -2\zeta\gamma & -1/J_0 \\ J_0\gamma^2 & 0 \end{bmatrix} \begin{bmatrix} z_1 \\ z_2 \end{bmatrix} = \begin{bmatrix} -4\zeta^2\gamma^2+\gamma^2 & 1/J_0 \\ 2\zeta\gamma^3 J_0 & 0 \end{bmatrix} \begin{bmatrix} \theta_1 \\ T_m \end{bmatrix} \quad \cdots\cdots (8)$$

$$\begin{bmatrix} \hat{\theta}_1 \\ \hat{T}_d \end{bmatrix} = \begin{bmatrix} z_1 \\ z_2 \end{bmatrix} + \begin{bmatrix} 2\zeta\gamma \\ -J_0\gamma^2 \end{bmatrix} \theta_1 \quad \cdots\cdots (9)$$

The transfer function of the observer mentioned above is expressed as follows:

$$\hat{\theta}_1 = \frac{s}{s^2+2\zeta\gamma+\gamma^2}\left(\frac{T_m}{J_0}+(s2\zeta\gamma+\gamma^2)\theta_1\right) \quad \cdots (10)$$

$$\hat{T}_d = \frac{\gamma^2}{s^2+2\zeta\gamma+\gamma^2}(T_m - s^2 J_0\theta_1) \quad \cdots\cdots (11)$$

4. Composition 1 of Control System

The block diagram of the case where the estimated disturbance data of the observer is fed back by the sign which negates the disturbance is provided in **Fig.4**. Next, the pole of the observer is moved and an appropriate pole is searched for from the pole assignment method and the frequency characteristics. On the other hand, it is important to determine what data to be selected for the nominal inertia data J_0 for design. An example of numerical data is listed in **Table 2**.

The frequency characteristics of the primary side position/torque in case the nominal inertia data J_0 is set as J_{max} when the real inertia $J = J_1 + J_{2max}$ are shown in **Fig.5**, while the secondary side position/torque is shown in **Fig.6**. Figure 5 shows that the pole of the observer is arranged nominally to the single inertial system as it moves towards negative infinity. When a pole of medium degree is selected, the observer influences the resonance pole greatly but its influence over the anti-pole is rather weak. Thus, the anti-resonance characteristics are left almost untouched. Figure 6 indicates that the resonance characteristics once

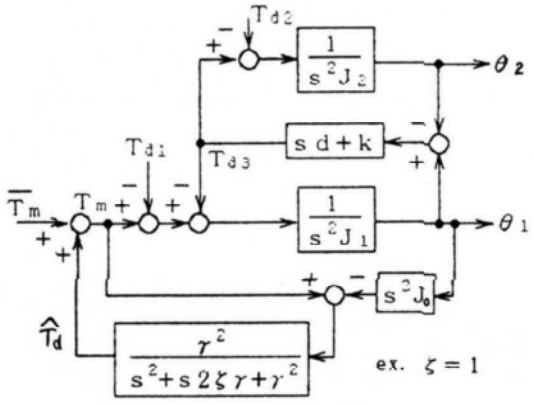

Fig. 4. 2-mass Model with Estimated Disturbance Feedback.

Table 2. Example of parameters range for servo system.

Item	Range of design data
Pole of observer $-\gamma$	$-1 \sim -500$
Nominal inertia data J_0	$1.25\text{-}1.64\times10^{-4}$ kgm²

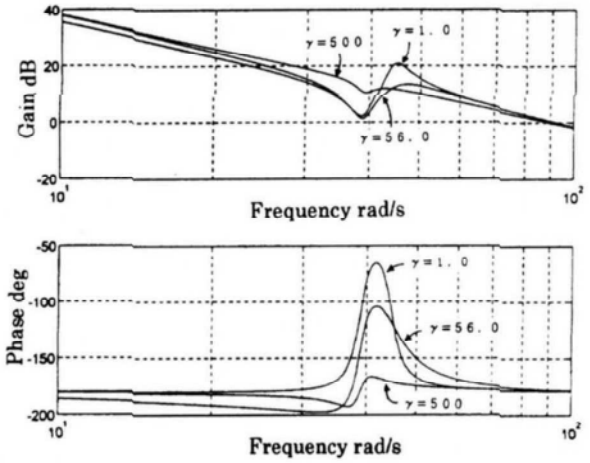

Fig. 5. Bode diagram for first side position/torque at J_0=J_{max}

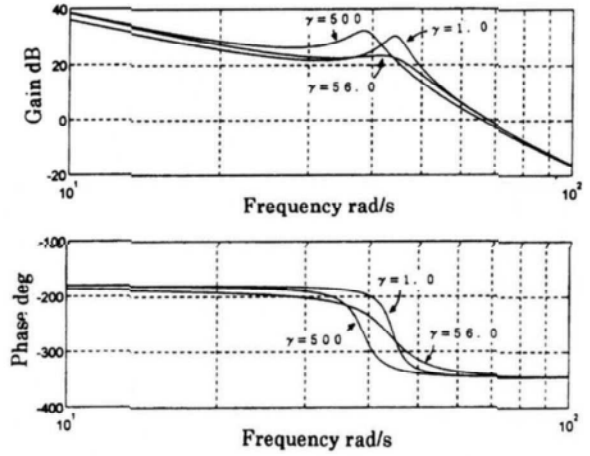

Fig. 6. Bode diagram for second side position/torque at J_0=-J_{max}.

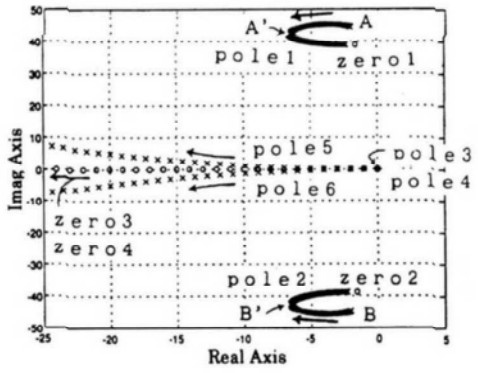

Fig. 7. Root locus plant with estimated disturbance data feedback.

attenuate but they are excited again on the low frequency side with the changes of the pole of the observer. This remains the same as the phenomenon already reported.[5] **Figure 7** shows the root locus related to Fig.5. However, the damping constant of the observer is set to 1, and the response frequency γ is made to fluctuate. As the negative pole ($-\gamma$) of the observer is changed to the negative direction by feeding back the estimated disturbance data, the two poles (poles 1 & 2) governing the resonance characteristics of the control system once move in the negative direction of the real axis and begin to move toward the zero points (zero 1 and zero 2) after changing the direction at the points A′ and B′. The two poles (poles 3 & 4) at the original point stay stationary but the remaining two poles (poles 5 & 6) are mutually complex conjugate and move toward the negative point at infinity. The same is true of the two zero points (zeros 3 and 4). The zero points (zeros 1 and 2) as related to the anti-resonance characteristics do not appear in the transfer function on the secondary side instead, they have a zero point ($-k/d$,0) but have nothing to do with motion. Consequently, pole-zero cancelling (pole 1 and zero 1, pole 2 and zero 2) shown in Fig.7 appears on the primary side alone, and the assignment of two poles (poles 1 and 2) on the secondary side determines the vibration characteristics. As a result, an observer is designed with the real axis composition of the poles 1 and 2 at a minimum, the control system will have great dampening characteristics. The design parameter γ will be shown in the Eq.(12). This represents γ when the maximum value of the absolute value of the reflex force T_{d3} in $\omega = 0 \sim \infty$ becomes the minimum.

$$\gamma = \left\{ \gamma \left| \min \left\| \omega = 0 - \infty \; \omega^2 J_2 \left(\frac{\theta_2(j\omega)}{\overline{T}_m(j\omega)} \right) \right\| \right|_\infty \right\} \quad . \quad (12)$$

In case of numerical values as an example, the parameter which satisfies the conditions $\gamma = 56.0$.

Next, the nominal inertia J_0 used in designing the observer is fluctuated and a comparison of characteristics is made to obtain the most appropriate inertia data. **Figure 8** indicates the root locus related to the transfer function of the position θ_1 on the primary side against the nominal torque input T_m in case the estimated disturbance data are feedback. Wherein, $\theta = 56.0$. In Fig.8, the positions of poles (poles 5 and 6) away from the imaginary axis change. whereas the poles (poles 1 and 2) and zeros (zero 1 and 2)which are close to the imaginary axis change very little. Subsequently, a difference in the selection of nominal inertia data at the time of design has not come to cause much of a change in characteristics.

5. Composition 2 of Control System

In order to compose the position control system, it is necessary to install a compensator on the external side of the feedback of the estimated disturbance data. In this report, this will be called the external compensator. In this connection, the problem is that the external compensator interferes with the compensating function of the estimated disturbance data inside, resulting in generating the characteristics contrary to the design. For instance, even if the observer pole is selected with the intent of improving the resonance characteristics on the second side, the external compensator in appropriately selected will enable the resonance characteristics to be conspicuous again, and there are cases when vibration is excited. In this report, a study will be made when the external compensator is of a PD type. When a control input Eq.(13) including the acceleration feed-forward is used, the control system will be as shown in **Fig.9**. At this point, a change in characteristics will be examined when the observer pole is fixed and the external compensator is changed. Based on the assumption that the observer has previously provided the object of control with the nominal inertia in an ideal manner, the gains K_p, K_d will be set to enable the position control system to be a dipole. The value of the design pole of the PD control system is set as $-\delta$.

$$T_m(s) = K_p(\theta_d - \theta_1) - K_d \hat{\dot{\theta}}_1 + \hat{T}_d(s^2 J_1 + sK_d)\theta_d$$

$$= \frac{(s^2 + 2\zeta\gamma + \gamma^2)(s^2 J_1 + sK_d + K_p)}{s\{s + (2\zeta\gamma + K_d/J_0)\}} \theta_d$$

$$- \frac{s^2(K_p + 2\zeta\gamma K_d + J_0\gamma^2) + s(K_d\gamma^2 + 2\zeta\gamma K_p) + K_p\gamma^2}{s\{s + (2\zeta\gamma + K_d/J_0)\}} \theta_1$$

. . . . . (13)

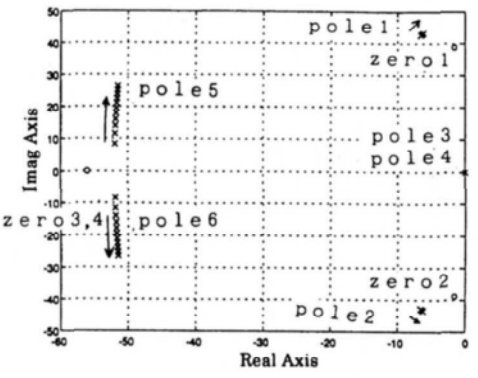

Fig. 8. Root locus of 1st side position/modified torque command for difference of nominal inertia data.

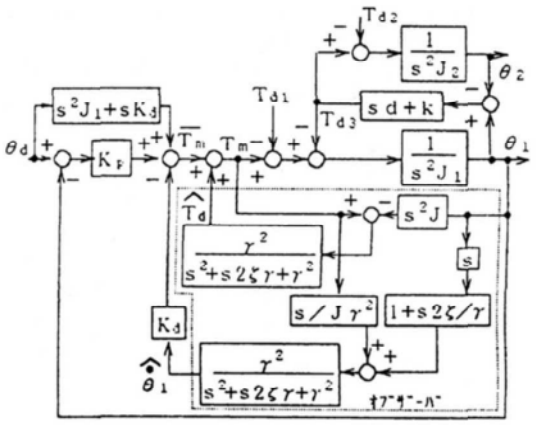

Fig. 9. Position control system block diagram.

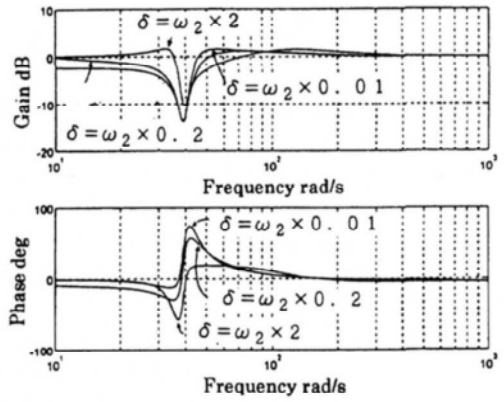

Fig. 10. Bode diagram for 1st side position/position reference at γ=–56.01.

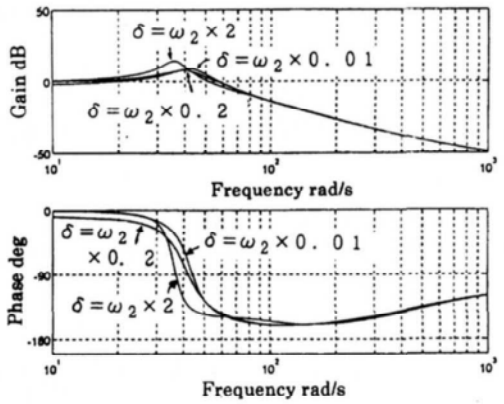

Fig. 11. Bode diagram for 2nd side position/position reference at γ=–56.01.

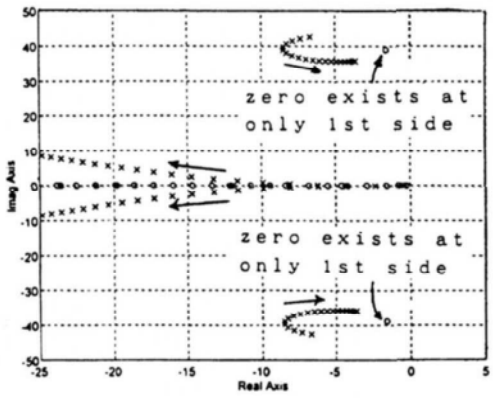

Fig. 12. Root locus of position control system at γ=–56.01.

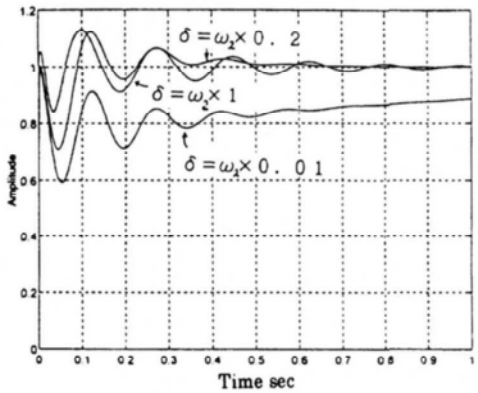

Fig. 13. Step response of 1st side position for fluctuations of servo parameters.

Figure 10 presents an example of the frequency characteristics of the position θ_1 on the primary side corresponding to the position command data θ_d. Wherein $\gamma = 56.0$ When the control pole $-\delta$ is changed in the negative direction, the anti-resonance characteristics attenuate, wherein $\gamma = 56.0$. As far as Fig.10 is concerned, the greater the value of $\delta(> 0)$ is, the better it will be. **Figure 11** illustrates the closed loop characteristics G_c of the position on the secondary side. It will be clear that it is easier to vibrate even if the pole of the observer is properly selected, depending upon the external compensator. With vibration control, δ which satisfies the Eq.(14) will be numerically calculated. The equation indicates δ when the maximum value of the absolute value of G_c at $\omega = 0 \sim \infty$ becomes the minimum. When numerically shown; $\delta = \omega_2 \times 0.20$.

$$\delta = \left\{ \delta \,|\min\|_{\omega=0-\infty} G_c(j\omega)\|_\infty \right\} \quad \cdots\cdots\cdots \quad (14)$$

Where, G_c = Closed loop transfer function of position control system. Next, the root locus corresponding to Fig.10 is shown in **Fig.12**. This makes it possible to verify the appropriateness of the Eq.(14). In Fig.10, the acceleration feed-forward gain has been set as the inertia data on the primary side. This is due to the fact that the nominal inertia data in the high frequency range are identical with the characteristics of the inertia data on the first side. If set to the inertial sum, the feed-forward in the high frequency range will be excessive. As a next step, the excessive charac-

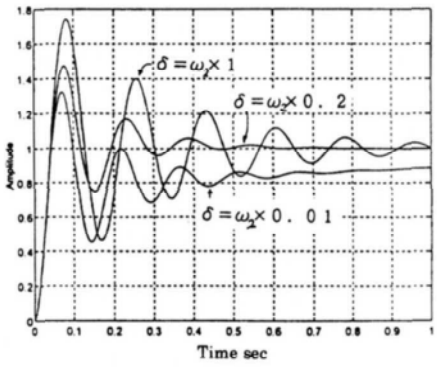

Fig. 14. Step response of 2nd side position for fluctuations of servo parameters.

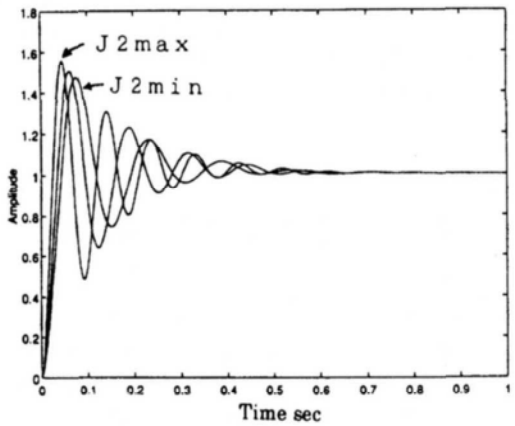

Fig. 15. Step response of 2nd side position for servo system with fluctuation of inertia.

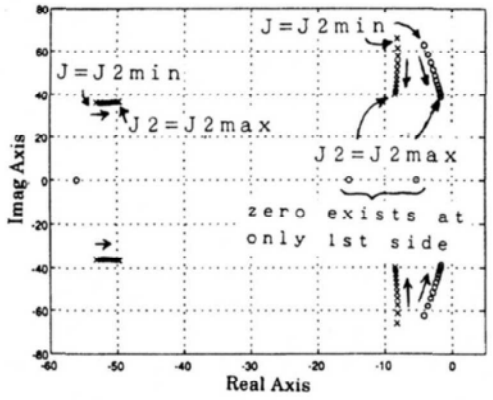

Fig. 16. Root locus for servo system with fluctuation of inertia.

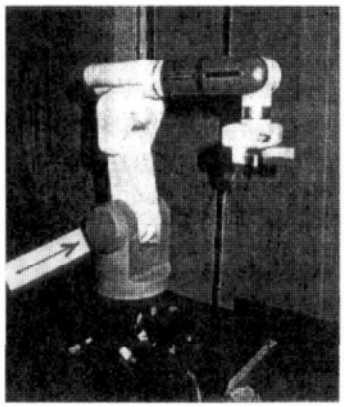

Fig. 17. Vertically articulated robot R50 for examination.

teristics will be evaluated to make sure that the vibrations are controlled by a proper parameter. Next, the excess characteristics against fluctuations in inertia will be evaluated. **Figure 15** indicates the step response when the inertia on the secondary side fluctuates from the minimum value to 1.5 times the maximum value when $\gamma = 56.0$ and $\delta = \sqrt{(J_{2max}/k)} \times 0.20$. The amplitude and the frequency of vibration are fluctuating but are fast attenuating at the same time. Likewise, the root locus at the time of fluctuation of the inertia is shown in **Fig.16**. The distance to the imaginary axis of the pole close to the imaginary axis will change little and it will be the control system with a high robustness.

6. Experimental Results

In order to verify the results mentioned above, an experiment was conducted. The robot used was a vertical articulated robot R50 (**Fig.17**) made by Seiko Seiki Co., Ltd. with the controller SA3000, of which the specifications are listed in **Table 3**. The axis used in the experiment is the vertical motion axis (second axis) which is the second axis from the base side and an approximate value of the parameter of a rough calculation of the motor axis is identical to **Table 1**. The motion back and forth between the two points where vibration was generated rather conspicuously was selected in the experiment, and the acceleration at the end of the robot and the position deflection of the motor axis were

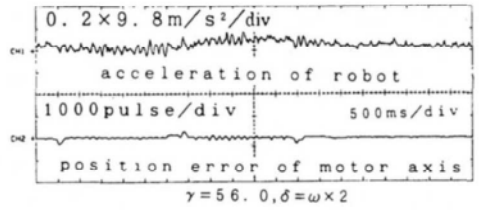

Fig. 18. Acceleration at end of robot and positioning error of motor axis at γ=56.01, $\delta=w_2\times0.2$.

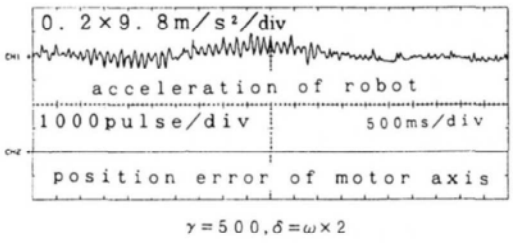

Fig. 19. Acceleration at end of robot and positioning error of motor axis at γ=500, $\delta=w_2\times0.2$.

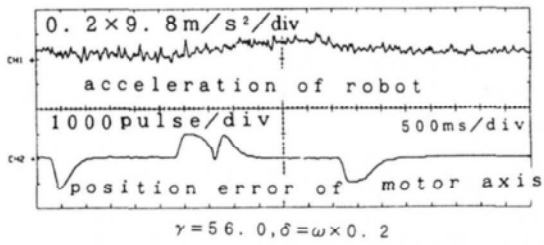

Fig. 20. Acceleration at end of robot and positioning error of motor axis at γ=56.01, $\delta=w_2\times0.2$.

Table 3. Specification of vertically articulated robot manipulator and controller.

Item	Data
Axes of manipulator	6
Payload of manipulator kg	6
Type of motors	AC servo motor
CPU, DSP for motion control	68 000, μPD 77230 A
Sampling time ms	1

measured. The former corresponds to the acceleration on the secondary side of an approximate model of the two-mass mechanism and was intended to evaluate the vibrations of the robot. The latter was intended to evaluate the traceability of the target value as related to the position on the primary side. To measure the velocity, the velocity pickup ($1V/9.8_{m.s^{-2}}$) was measured in the direction of revolution of the secondary axis at the end of the robot.

From **Fig.18** and **Fig.19**, a comparison was made of the differences of the parameters γ of the observer. When the acceleration waves in the upper section of each diagram were compared to find that the maximum value of acceleration showed no difference. However, as far as the peak-peak was concerned, the vibration in Fig.18 was controlled better. When attention was paid to the part of the frequency showing vibrations more conspicuously, Fig.18 indicates about 7Hz(= 44rad/s) and Fig.19 about 6.5Hz(= 40rad/s), indicating the characteristics close to the double inertia sys-

tem. On the other hand, when the deflections on the motor axis were compared, the position deflection in Fig.19 was low, whereas the vibrations were generated in Fig.18. The resolution per one rotation of the motor is 4.096 pulses. In **Fig.20**, aimed at controlling the vibrations of both the observer and the external compensator, it is clear that the vibrations are better controlled than those in Fig.18. On the other hand, it is clear that the position deflection at the motor axis has increased. The frequency remains almost identical to that in **Fig.19**. As discussed above, this experiment has revealed that in case emphasis is placed on controlling the vibrations at the end of the robot as related to the design of the proposed control system, it is possible to have the design to satisfy the control specification if the control parameters are obtained in accordance with the proposed procedures and the control parameters as shown in Fig.20 are used.

7. Conclusion

(1) The object of control has been approximated to the two-mass mechanism and the control system has been analyzed.

(2) The pole assignment of the observer aimed at controlling the two-mass mechanism has been set with the frequency characteristics at the time of feedback of the estimated disturbance data used as the standard of evaluation. With the nominal inertia data for design also set as a design variable, specific fluctuations have been evaluated.

(3) In order to utilize the result of (2) for controlling vibrations, it has been made clear that the compensator arranged on the outside of the feedback group by the observer should be designed properly.

(4) In order to evaluate the analytical results mentioned above, the experimental results have been presented for at evaluating the acceleration at the end of the robot in motion.

Acknowledgements
In concluding, I would like to express my appreciation to Prof. K. Ohnishi of Keio University and Prof. T. Mita of Tokyo Institute of Technology for their kind guidance and advice.

References:

1) A. Shimada, "Disturbance Torque and Velocity Estimated Observer Based Control System for Low-Stiffness Robot Manipulator," Journal of the Robotics Society of Japan , **10-7** (1992) 983.
2) A. Shimada, "Analyses of Estimation Error on Observer for Disturbance and Velocity," IEE Japan, **113-D**-7 (1993) 874.
3) K. Yuuki, T. Murakami and K. Ohnishi, "Vibration Restraint Control of the Double Inertia Resonance System by Resonant Ratio Control," IEE Japan, **113-D**-10 (1993) 1162.
4) A. Shimada and H. Fukami, "Design of the 2-degree of Freedoms Servo System for Low-stiffness for Robot with Fluctuation of Inertia and Friction," '94 Robotics Mechatronics Conference, The Japan Society of Mechanical Engineers (1994) 711.
5) M. Iwata, "Response-type Vibration Restraint Control Based on Parameter Fixation of the Double Inertia Resonance System," IIC-94-11, IEE Japan (1994) 87.

This article appeared in English in Journal of the Japan Society for Precision Engineering , Vol. 61, No. 9, pp. 1332-1336, September 1995.

Name:
Akira Shimada

Affiliation:
Assistant Manager, Research & Development Dept., Seiko Seiki Co., Ltd.

Address:

Brief Biographical History:
1983 - Joined Seiko Instruments Inc.
1992 - Changed for Seiko Seiki Co., Ltd.,
1996 - Received Ph.D in Engineering from Keio Univ.

Main Works:
- "The Digital Observer which Estimates Disturbance and Velocity", IEE Japan, 113-D-4, pp.487-494, '93.

Membership in Learned Societies:
- The Robotics Society of Japan (RSJ)
- The Society of Instrument and Control Engineers (SICE)
- The Institute of Electrical Engineers of Japan (IEEJ)
- The Japan Society for Precision Engineering (JSPE)